An ultra-compact cross/bar optical routing switch using two polymer electro-optic microrings*

SONG Qiang (宋强), **ZHENG Chuan-tao** (郑传涛)**, **LIANG Lei** (梁磊), **LUO Qian-qian** (罗倩倩), **MA Chun-sheng** (马春生), **ZHANG Da-ming** (张大明), **and WANG Yi-ding** (王一丁)

State Key Laboratory on Integrated Optoelectronics, College of Electronic Science and Engineering, Jilin University, Changchun 130012, China

(Received 11 April 2013)

A 2×2 cross/bar polymer electro-optic (EO) routing switch is proposed, which is composed of two passive channel waveguides and two active EO polymer microrings with bending radius of only 13.76 μm. Detailed structure, theory and formulation are provided to characterize the output power of the switch. For obtaining fundamental mode propagation, small bending loss and phase-matching between channel waveguide and microring resonator (MRR) waveguide, the structural parameters are optimized under the wavelength of 1550 nm. Analyses and simulations on output power and output spectra indicate that a switching voltage of 5 V is desired to realize the exchange between cross state and bar state, the crosstalk under cross state and that under bar state are about −28.8 dB and −39.9 dB, respectively, and the insertion losses under these two states are about 2.42 dB and 0.13 dB, respectively. Compared with our four EO switches reported before, this device possesses ultra-compact size of 0.233 mm×0.233 mm as well as low crosstalk and insertion loss, and therefore it can serve as a good candidate for constructing large-scale optical routers or switching arrays in photonic network-on-chip (NoC).

Document code: A **Article ID:** 1673-1905(2013)05-0337-5

DOI 10.1007/s11801-013-3072-9

The core part of a photonic network-on-chip (NoC) is an on-chip photonic interconnection network, which is composed of passive waveguides and optical routers[1], and it has better performance to meet various needs. A basic 2×2 switching element and the reasonable architecture are the first step for constructing optical routers. Previously, by using directional coupler (DC), Y-fed coupler, Mach-Zehnder interferometer (MZI), multimode interference (MMI), etc, different 2×2 polymer electro-optic (EO) switches have been reported[2-6]. However, they are found to be unsuitable to form large-scale switching arrays because of the long waveguide and electrode, and scalability may be a serious problem. Among the available optical switches, microring resonator (MRR) based optical switches are typically preferred due to their ultra-compact size, simple-mode resonances and ease of phase-matching between an MRR and its coupling waveguides[7]. Besides, the MRR structure is more convenient for building large switching arrays by cascading fundamental elements. Therefore, in recent years, using EO material and the microring with filtering function, some EO MRR switches[8-10] were reported. In this paper, by using two MRRs, a compact 2×2 cross/bar EO routing switch is designed and optimized, and by tuning the applied voltage on the two microrings, favorable routing operation is realized with crosstalk lower than −28.8 dB and −40 dB.

Fig.1(a) and (b) depict the structure of the cross/bar EO routing switch, and the cross-section view over the coupling region between the MRR waveguide and channel waveguide. The device consists of a horizontal rectangular waveguide, a vertical rectangular waveguide and two microrings with the same radius. The distance between the input port and its neighboring coupling point and that between the output port and its neighboring coupling point are both L_1=100 μm. As shown in Fig.1(b), the electrode is only deposited upon the MRR waveguide, and the channel waveguide is passive without electrode. Due to the bending effect, the mode propagation constant is different from that of the straight waveguide with the same size[11]. Therefore, under the case without applying voltage, for obtaining the same mode propagation constant, the two core widths of the MRR waveguide and channel waveguide are slightly different, defined as w_r and w_c, respectively. Also, the under cladding layer thickness of the channel waveguide is slightly larger than that

* This work has been supported by the National Natural Science Foundation of China (Nos.61107021, 61177027 and 61077041), the Ministry of Education of China (Nos.20110061120052 and 20120061130008), the China Postdoctoral Science Foundation Funded Project (Nos.20110491299 and 2012T50297), the Special Funds of Basic Science and Technology of Jilin University (Nos.201103076 and 200905005), and the Science and Technology Department of Jilin Province of China (No.20130522161JH).

** E-mail: zhengchuantao@jlu.edu.cn

of the MRR waveguide, and their relation is $t_{2c}=t_2+t_3$, where t_2 and t_3 are the under cladding thickness and electrode thickness of the MRR waveguide, respectively. When t_2 is taken sufficiently large, a small increase of the under cladding thickness has no influence on mode constant.

During design, the resonance wavelength is selected as λ_0=1550 nm; the refractive index, amplitude loss coefficient and EO coefficient of the core material are n_{10}=1.59, α_{10}=0.25 dB/cm and γ_{33}=68 pm/V, respectively[12]; the refractive index and amplitude loss coefficient are n_{20}=1.461 and α_{20}=0.25 dB/cm, respectively[13]; the electrode material is Au, and its refractive index and bulk extinction coefficient are n_{30}=0.19 and κ_{30}=6.1, respectively[14]; the left and right cladding layer materials are both air, and its refractive index and amplitude loss coefficient are n_{40}=1 and α_{40}=0, respectively. The high index contrast n_{10}–n_{40} between EO core and left/right cladding layer allows small bending radius and device size.

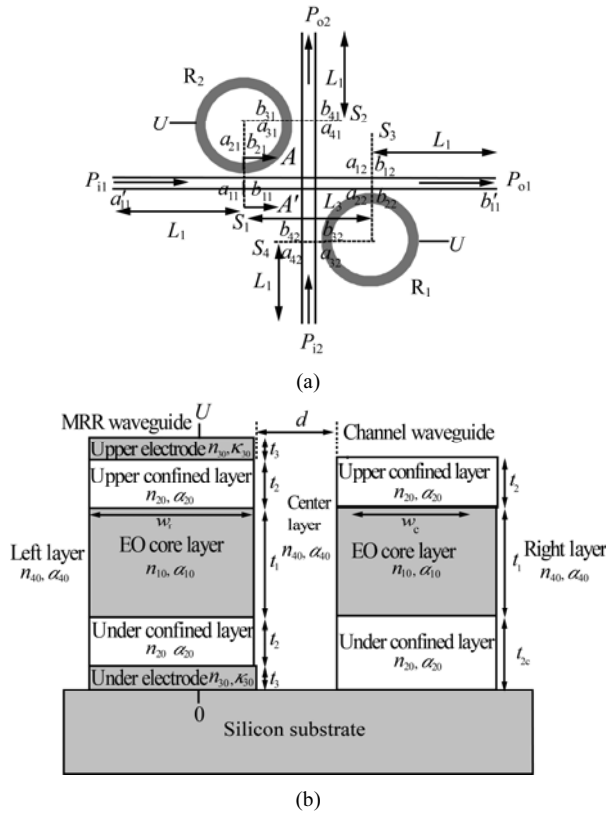

Fig.1 (a) Structure of the cross/bar MRR EO routing switch; (b) Cross-section view over the coupling region between the MRR waveguide and the channel waveguide

Let the light with resonance wavelength input into the horizontal waveguide. (1) When the applied voltage U on the two microrings R_1 and R_2 is zero, the output power from the vertical waveguide becomes the maximum, whereas the output power from the parallel waveguide becomes the minimum. This state is named as the cross state. (2) When a voltage is applied on R_1 and R_2, the core refractive index of the MRR waveguide is changed, and the mode propagation constant reveals mismatch with that of the channel waveguide, therefore the output power values from the horizontal and vertical waveguides are changed. With a suitable voltage (named as the switching voltage), the output power from the vertical waveguide becomes the minimum, whereas the output power from the parallel waveguide becomes the maximum. This state is named as the bar state.

The refractive index change of the MRR EO core material resulting from the applied voltage U is

$$\Delta n_{10}=\frac{1}{2}n_{10}^3 r_{33}E_1=\frac{n_{10}^3 n_{20}^2 r_{33}U}{2(2n_{10}^2 t_2+n_{20}^2 t_1)}. \tag{1}$$

Then the refractive index of the EO core material can be changed from n_{10} to $n_{10}+\Delta n_{10}$, and the indices of other materials are not changed, since they are non-EO materials.

For the microring R_2, define a_{11} as the input light amplitude into the coupling point with the horizontal waveguide, b_{11} as the output light amplitude from the coupling point with the horizontal waveguide, and the other amplitudes including a_{21}, b_{21}, a_{31}, b_{31}, a_{41} and b_{41} are also labeled in Fig.1(a). For the microring R_1, define a_{12} as the input light amplitude into the coupling point with the horizontal waveguide, b_{12} as the output light amplitude from the coupling point with the horizontal waveguide, and the other amplitudes including a_{22}, b_{22}, a_{32}, b_{32}, a_{42} and b_{42} are also labeled in Fig.1(a). Over the cross-section planes S_1, S_2, S_3 and S_4, we can obtain the following relations among the above amplitudes as

$$b_{11}=ta_{11}-\mathrm{j}\kappa b_{31}\exp(-\mathrm{j}\varphi_1), \tag{2}$$
$$b_{21}=-\mathrm{j}\kappa a_{11}+tb_{31}\exp(-\mathrm{j}\varphi_1), \tag{3}$$
$$b_{31}=-\mathrm{j}\kappa a_{41}+tb_{21}\exp(-\mathrm{j}\varphi_2), \tag{4}$$
$$b_{41}=ta_{41}-\mathrm{j}\kappa b_{21}\exp(-\mathrm{j}\varphi_2), \tag{5}$$
$$b_{12}=ta_{12}-\mathrm{j}\kappa b_{32}\exp(-\mathrm{j}\varphi_2), \tag{6}$$
$$b_{22}=-\mathrm{j}\kappa a_{12}+tb_{32}\exp(-\mathrm{j}\varphi_2), \tag{7}$$
$$b_{32}=tb_{22}\exp(-\mathrm{j}\varphi_1), \tag{8}$$
$$b_{42}=-\mathrm{j}\kappa b_{22}\exp(-\mathrm{j}\varphi_1), \tag{9}$$
$$a_{41}=b_{42}\exp(-\mathrm{j}\psi_2), \tag{10}$$
$$a_{12}=b_{11}\exp(-\mathrm{j}\psi_2), \tag{11}$$
$$a_{42}=0, \tag{12}$$

and the phases can be expressed as

$$\varphi_1=\frac{3}{2}\pi R(\beta_R-\mathrm{j}\alpha_R), \tag{13}$$
$$\varphi_2=\frac{1}{2}\pi R(\beta_R-\mathrm{j}\alpha_R), \tag{14}$$
$$\psi_2=L_3(\beta_C-\mathrm{j}\alpha_C), \tag{15}$$

where $\beta_C=\beta_0$ is the mode propagation constant of the channel waveguide, $\beta_R=\beta_0$ is that of the MRR waveguide under U=0, $\beta_R=\beta_U=\beta_0+\Delta\beta$ is that of the MRR waveguide under $U\neq0$, and $\Delta\beta$ is the propagation constant variation induced by the index change of Δn_{10}. α_C and α_R are mode

loss coefficients of the channel waveguide and MRR waveguide, respectively.

Finally, we derive the transfer coefficients of the device as

$$M=\frac{b_{12}}{a_{11}}=\frac{t^2\left\{f_1-k^2\exp[-\mathrm{j}(\varphi_1+\varphi_2)]\right\}}{f_2}\times \frac{\exp(-\mathrm{j}\psi_2)\{1-\exp[-\mathrm{j}(\varphi_1+\varphi_2)]\}}{f_2}, \tag{16}$$

$$N=\frac{b_{41}}{a_{11}}=-\frac{k^2 f_2\exp(-\mathrm{j}\varphi_2)}{f_1 f_2}- \frac{t^2k^2\exp\left[-\mathrm{j}(\varphi_1+2\psi_2)\right]\left\{f_1-k^2\exp\left[-\mathrm{j}(\varphi_1+\varphi_2)\right]\right\}^2}{f_1 f_2}, \tag{17}$$

where

$$f_1=1-t^2\exp\left[-\mathrm{j}(\varphi_1+\varphi_2)\right], \tag{18}$$

$$f_2=f_1^2-k^4\exp\left[-\mathrm{j}(2\varphi_1+2\psi_2)\right]\times \left\{f_1+t^2\exp\left[-\mathrm{j}(\varphi_1+\varphi_2)\right]\right\}. \tag{19}$$

Define the input light amplitude into the horizontal waveguide as $a_{11}^{'}$, the output light amplitudes from the horizontal waveguide and vertical waveguide as $b_{12}^{'}$ and $b_{41}^{'}$, respectively, and they can be written as

$$a_{11}^{'}=a_{11}\exp(\mathrm{j}\psi_1), \tag{20}$$

$$b_{12}^{'}=b_{12}\exp(-\mathrm{j}\psi_1), \tag{21}$$

$$b_{41}^{'}=b_{41}\exp(-\mathrm{j}\psi_1), \tag{22}$$

where $\psi_1=L_1(\beta_C-\mathrm{j}\alpha_C)$. Finally, the power transfer functions can be expressed as

$$|B|^2=\left|\frac{b_{12}^{'}}{a_{11}^{'}}\right|^2=\left|\frac{b_{12}}{a_{11}}\exp(-\mathrm{j}2\psi_1)\right|^2=\left|M\exp(-\mathrm{j}2\psi_1)\right|^2, \tag{23}$$

$$|D|^2=\left|\frac{b_{41}^{'}}{a_{11}^{'}}\right|^2=\left|\frac{b_{41}}{a_{11}}\exp(-\mathrm{j}2\psi_1)\right|^2=\left|N\exp(-\mathrm{j}2\psi_1)\right|^2, \tag{24}$$

and the output power functions in dB form are

$$P_{o1}=10\log_{10}\left(|B|^2\right), \tag{25}$$

$$P_{o2}=10\log_{10}\left(|D|^2\right). \tag{26}$$

Since the applied external electric field is along the *y* direction, for increasing EO overlap integral, the selected propagation mode is E_{00}^{y}, whose main field components are E_y and H_x. For the active MRR waveguide, by using the technique proposed in Ref.[2], the upper/under cladding thickness and electrode thickness are optimized as t_2=2.0 μm and t_3=0.15 μm, respectively, in this case, the upper/under cladding and upper/under electrode can both be treated as half-infinite, and the absorption loss of electrode can be decreased to the minimum value. Without considering the influence of bending on mode constants, Fig.2(a) shows the relation of effective refractive indices of E_{00}^{y}, E_{01}^{y} and E_{10}^{y} modes versus MRR waveguide core width w_r, where the thickness and width of the core are equal, i.e., $w_r=t_1$. It can be found that the single mode condition is 1.2 μm $<w_r=t_1<$2.1 μm, and here we select $w_r=t_1$=1.7 μm. The influence of bending on refractive index of E_{00}^{y} mode is further considered, as shown in Fig.2(a), where the bending radius is R=13.76 μm. As can be seen, the mode index is increased because of bending, and the mode effective index is $n_{c,R}$=1.5243 when $w_r=t_1$=1.7 μm.

For the channel waveguide, the core thickness is equal to that of the MRR waveguide, which is 1.7 μm. When the applied voltage is zero, the mode effective indices of the two waveguides should be identical. Fig.2(b) also presents the curve of effective index of E_{00}^{y} mode versus the channel waveguide core width w_c. For making sure the two effective indices of MRR waveguide and channel waveguide to be identical, we obtain w_c=2.03 μm.

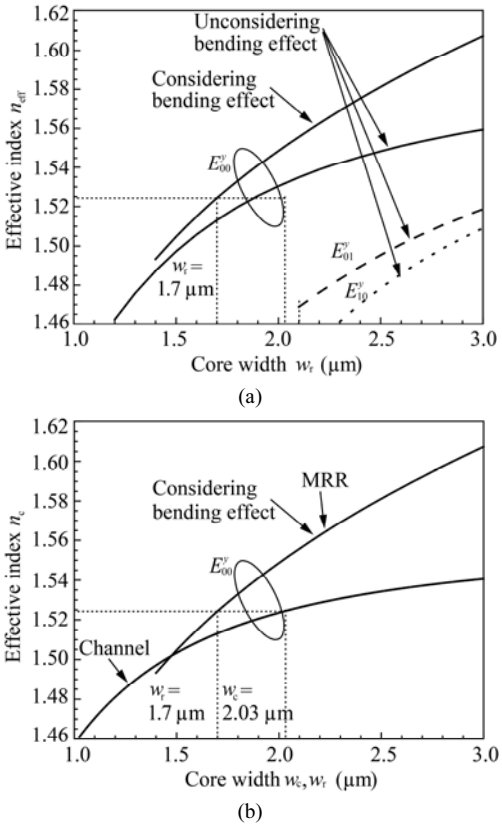

Fig.2 (a) Effective refractive indices of E_{00}^{y}, E_{01}^{y} and E_{10}^{y} modes versus core width of MRR waveguide with and without considering bending effect; (b) Effective refractive index of E_{00}^{y} mode versus core width of channel waveguide and core width of MRR waveguide considering bending effect

The bending radius should satisfy the resonance condition

$$2\pi R n_{c,R}=m\lambda, \tag{27}$$

where m is the resonance order, and $n_{c,R}$ is the mode effective index which is also dependent on bending radius. Fig.3(a) shows the curves of fundamental mode effective index $n_{c,R}$ and bending radius R versus the resonance order m, where $w_r=t_1$=1.7 μm, and the upper/under clad-

ding is assumed to be half-infinite. As m increases, $n_{c,R}$ decreases and R increases. Properly, we select m=85, and the bending radius is determined to be R=13.76 μm.

On the other hand, the bending will cause extra power bending loss of the propagation mode along MRR waveguide. Fig.3(b) exhibits the effects of R on $n_{c,R}$ and power bending loss α_p. It can be observed that α_p decreases exponentially as the increase of R, and when R=13.76 μm, α_p drops below 10^{-4} dB/cm.

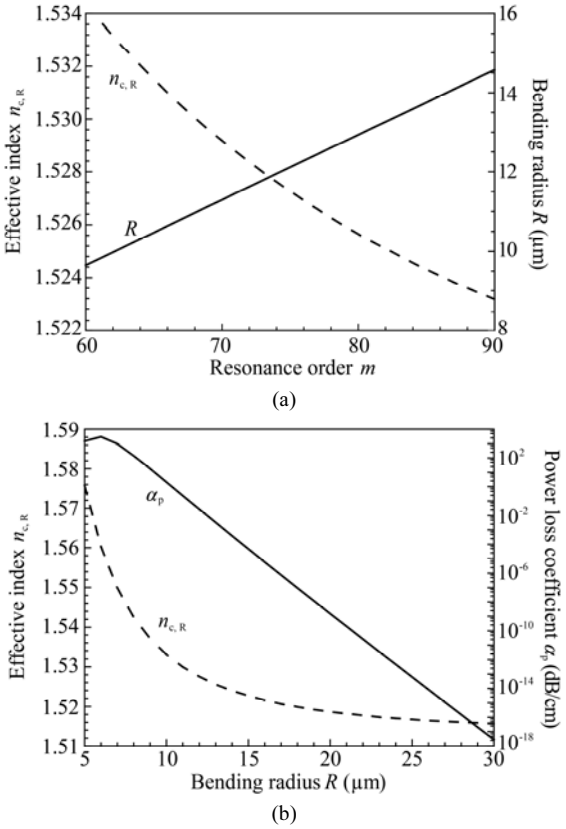

Fig.3 (a) Fundamental mode effective index $n_{c,R}$ and bending radius R versus resonance order m; (b) Effects of bending radius R on mode effective index $n_{c,R}$ and power bending loss coefficient α_p

The coupling coefficient between the MRR waveguide and channel waveguide is a key parameter of the device, which should be carefully selected during the design of the device. Fig.4 shows the effect of coupling gap d between the channel waveguide and MRR waveguide on the coupling coefficient κ_{CR}, where w_r=t_1=1.7 μm and w_c=2.03 μm. The gap cannot be taken too small, otherwise the fabrication accuracy may be a problem, whereas it cannot be taken too large, either, otherwise the coupling effect becomes too weak. Therefore, we choose d=0.14 μm, the corresponding coupling coefficient is κ_{CR} =0.08664, and the transmittance coefficient is $t_{CR}=\sqrt{1-\kappa_{CR}^2}=0.99624$.

The final optimized parameters are listed in Tab.1.

For the optimized device, let the light input the horizontal waveguide only, that is, $P_{i1}\neq 0$ and $P_{i2}=0$. By using Eqs.(25) and (26), under the resonance wavelength of 1550 nm, Fig.5(a) shows the curves of output power P_{o1} and P_{o2} versus the applied voltage on the two microrings R_1 and R_2. It can be found that when U=0 V, the device is operated at cross state. The insertion loss under this state is about 2.42 dB, and the crosstalk between the two ports is −28.8 dB. As the increase of the applied voltage, the mode mismatch between the channel waveguide and MRR waveguide is enhanced, the output power from the cross port drops, and the output power from the through port increases. When the applied voltage is 5.0 V, the crosstalk between the two ports is below −39.9 dB, and the insertion loss of the through port is about 0.13 dB.

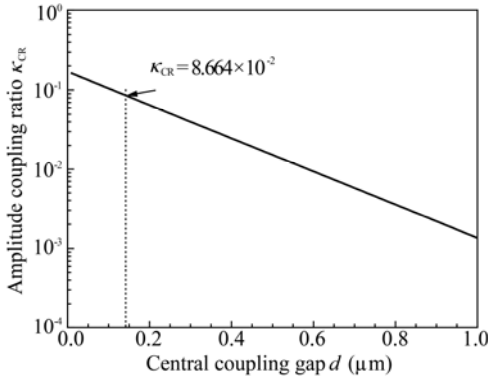

Fig.4 Effect of coupling gap d between the channel waveguide and MRR waveguide on the coupling coefficient κ_{CR}, where w_r=t_1=1.7 μm, and w_c=2.03 μm

Tab.1 Optimized parameters of the MRR EO switch

Parameter	Value	Parameter	Value
Core thickness t_1	1.70 μm	Resonance order m	85
Core width w_c	2.03 μm	Ring radius R	13.76 μm
Core width w_r	1.70 μm	Transmittance coefficient t_{CR}	0.99624
Buffer thickness t_2	2.00 μm	Coupling coefficient κ_{CR}	0.08664
Electrode thickness t_3	0.15 μm	Coupling gap d	0.14 μm

Under the applied voltages of 0, 5 V and 10 V, Fig.5(b) presents the curves of output power P_{o1} and P_{o2} from the cross port and through port versus the light wavelength. It can be found that under U=0 V and λ=1550 nm, the input power into the horizontal waveguide will fully output from the cross port through the coupling with microrings, the device operates at cross state, and the crosstalk is less than −28.8 dB. Under U=5 V, the output power of the cross port drops from point a to d, and that of the bar port increases from point b to c. This state is named as bar state, and the crosstalk is less than −39.9 dB. Under U=10 V, the crosstalk is lower than that under U=5 V, which is below −50 dB.

As shown in Tab.2, we make a comparison on the performance (including switching voltage, insertion loss and crosstalk under cross and bar states, and the total length of the core part of the device) of this 2×2 cross/bar MRR switch and our previously reported 2×2 or 1×2 EO switches based on directional coupler (DC), Y-fed cou-

pler, MZI and MMI-MZI structures. It can be found that the total length of this device is only 0.233 mm, which is much shorter than those of other four devices, and because of short waveguide length, this device reveals low insertion loss extremely at bar state. This device also has competitive crosstalk compared with other four switches, which is −28.8 dB and −39.9 dB at the cross and bar states, respectively.

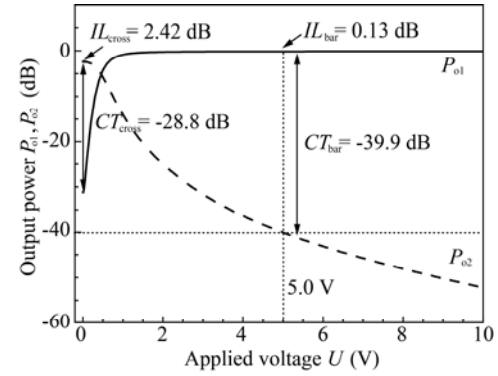

(a)

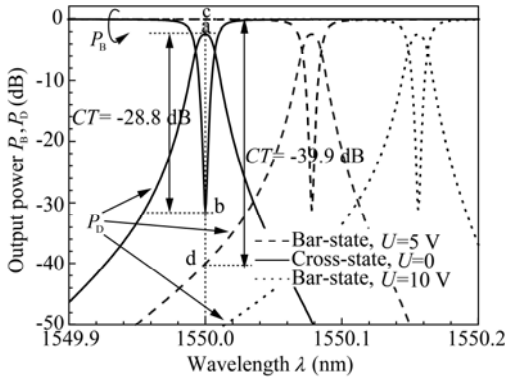

(b)

Fig.5 (a) Curves of output power P_{o1} and P_{o2} versus the applied voltage U on the two microrings R_1 and R_2; (b) Curves of output power P_{o1} and P_{o2} from the cross port and through port versus the light wavelength, where U = 0, 5 V and 10 V

Tab.2 Comparison of this switch and our previously reported three polymer EO switches

Structure	U_s (V)	IL_{bar}, IL_{cross} (dB)	CT_{bar}, CT_{cross} (dB)	L_{total} (mm)
Directional coupler[2]	1.645	1.98, 1.98	<–30, <–30	4.139
Y-fed coupler[3]	1.783	1.42, 1.42	<–30, <–30	3.126
MZI[5]	2.234	2.64, 2.64	<–30, <–30	5.049
MMI-MZI[4]	1.375	3.75, 3.75	<–42, <–42	5.000
MRR (this paper)	5.000	0.13, 2.42	<–39.9, <–28.8	0.233

As a conclusion, in terms of coupled mode theory, microring resonance theory and electro-optic modulation theory, a 2×2 cross/bar polymer EO switch is proposed by using two channel waveguides and two electro-optic microrings. Device structure is presented, and theory and formulation are derived to characterize the output power of the switch. In order to realize fundamental mode propagation, small bending loss and mode effective refractive index match between channel waveguide and MRR waveguide, the device structure is optimized under 1550 nm wavelength. A switching voltage of 5 V is desired to change the operation states, the crosstalks under cross state and bar state are about −28.8 dB and −39.9 dB, respectively, and the insertion losses under these two states are about 2.42 dB and 0.13 dB, respectively. Compared with our four EO switches reported before, this device possesses the ultra-short length of 0.233 mm, which can serve as a good switching element for constructing large-scale optical routers or switching arrays in next generation phonic NoC.

References

[1] A. W. Poon, F. Xu and X. Luo, Cascaded Microresonator-based Matrix Switch for Silicon On-chip Optical Interconnect, Proc. IEEE **97**, 1216 (2009).

[2] C. T. Zheng, C. S. Ma, X. Yan, X. Y. Wang and D. M. Zhang, Opt. Commun. **281**, 3695 (2008).

[3] C. T. Zheng, C. S. Ma, X. Yan, X. Y. Wang and D. M. Zhang, J. Mod. Opt. **56**, 615 (2009).

[4] C. T. Zheng, C. S. Ma, Z. C. Cui, X. Yan, D. M. Zhang and C. W. Tian, Opt. Quant. Electron. **42**, 327 (2011).

[5] C. T. Zheng, C. S. Ma, X. Yan, X. Y. Wang and D. M. Zhang, Opt. & Laser Technol. **42**, 457 (2010).

[6] C. T. Zheng, C. S. Ma, X. Yan, Z. C. Cui and D. M. Zhang, Appl. Phys. B **102**, 831 (2011).

[7] P. Dong, S. Liao, H. Liang, N. N. Feng, W. Qian, R. Shafiiha, D. Z. Feng, G. L. Li, X. Z. Zheng, J. Cunningham, A. V. Krishnamoorthy and M. Asghari, Proceedings of SPIE **7944**, 794403 (2011).

[8] G. B. Lee, A. Biberman, N. Sherwood-Droz, C. B. Poitras, M. Lipson and K. Bergman, J. Lightwave Technol. **27**, 2900 (2009).

[9] S. Y. Cho and R. Soref, Opt. Exp. **16**, 13304 (2008).

[10] C. Li, X. Luo and A. W. Poon, Semicond. Science Technol. **23**, 064010 (2008).

[11] A. Melloni, F. Carniel, R. Costa and M. Martinelli, J. Lightwave Technol. **19**, 571 (2001).

[12] G. Y. Xu, Z. F. Liu, J. Ma, B. Y. Liu, S. T. Ho, L. Wang, P. W. Zhu, T. J. Marks, J. D. Luo and A. K. Y. Jen, Opt. Exp. **13**, 7380 (2005).

[13] C. Pitois, S. Vukmirovic, A. Hult, D. Wiesmann and M. Robertsson, Macromolecules **32**, 2903 (1999).

[14] W. G. Driscoll and W. Vaughan, Handbook of Optics, New York: McGraw-Hill, 7 (1978).